Void fraction measurement based on electromagnetic wave sensor

Zhiyue Zhao[1,2], Longlong Wang[3], Xiaoting Li[1], Jing Wang[3], Liqiang Guo[3]

[1]*The College of Physics Science and Technology, Hebei University, 071002, Baoding, China.*
[2]*College of Mechanical and Electrical Engineering, Cangzhou Normal University, 061001, Cangzhou, China.*
[3]*Hebei Baisha Tobacco Co., LTD Baoding Cigarette Factory, 071000, Baoding, China*

E-mail (Jing Wang, Liqiang Guo): bdwj881111@126.com, glq13400238651 @126.com;

Abstract

Gas-liquid two-phase flow is an unavoidable energy flow phenomenon in industries, and void fraction measurement is a crucial challenge in the two-phase flow. In the study, the coaxial line phase sensor is designed base on electromagnetic wave transmission principle, by which void fraction of the slug and stratified flow was acquired. The void fraction measured by new coaxial has a well time-domain and Probability Density Functions (PDF) distribution characteristics, four typical models with different physical backgrounds were selected to evaluate the measured values of the sensors. The mean absolute errors (MAPE) were 7.85%, 24.41%, 7.22%, and 15.44% for slug flow, and 12.31%, 6.46%, 12.68%, and 2.95% for stratified flow. The results indicated that the coaxial line phase sensor has well measurement accuracy and not limited by the flow regime.
Keyword: Coaxial Sensor, void fraction, Dielectric constant, flow regime

1. Introduction

Gas-liquid two-phase flow is an unavoidable energy flow phenomenon in petrochemical, nuclear and aerospace industries, especially in the petrochemical field involving the extraction, transportation, storage and processing of oil and natural gas[1]. The measurement of the void fraction is a key parameter in the study of two-phase flows, as it is related to the calculation of mass and heat transfer, pressure drop and the design of processes and equipment in the production[2].

Due to the high coupling of gas and liquid phases, and the complex and variable flow conditions caused by pressure and flow rate, the measurement of void fraction has been an urgent problem in industrial production and scientific research. Numerous researchers and scholars have carried out research on developing sensors and measurement method, there are mainly optical[3, 4], acoustic [5, 6], nuclear radiation [7, 8] and electrical [9, 10] methods for void fraction measurement currently. Optical method is mainly divided into camera method [3], optical probe method [4]. The optical method requires transparent measurement environment and is easily disturbed by the external environment. Acoustic method is method is difficult to achieve quantitative analysis in the field of two-phase flow and is expensive. The application of radiometric methods in industrial sites is limited due to radioactivity and extremely high safety protection standards. Electrical methods are mainly divided into conductivity [9] and capacitance method [10], in which the probe is in contact with the fluid media and is susceptible to corrosion leading to a decrease in measurement accuracy. Capacitive method needs to arrange capacitive sensors around the pipe to measure the water content through fluid dielectric constant changes. The main research hotspot is the capacitive tomography imaging, but the technology requires a complex structure and a large number of high-speed computing circuit.

Coaxial wire is a two-conductor transmission line consisting of two inner and outer conductors and dielectric in the middle. It has the advantages of low cost, strong anti-interference, stable signal, and not easy to leak, and can complete the transmission of high frequency and very high frequency electromagnetic waves [11]. Coaxial line electromagnetic wave sensors have the same measurement principle with capacitive sensors, which use dielectric properties of the mixed media to achieve the measurement of gas and liquid components [12]. The difference is the electromagnetic wave measurement technique also utilizes the polarization characteristics of gas-liquid at higher frequencies, which not only overcomes the deficiency of low resolution of capacitive sensors, but also increases the polarization loss of conducting media [13].

In this paper, the sensor is designed base on the transmission characteristics of electromagnetic wave in the coaxial line, utilizing the phase difference when the gas-liquid medium flows through the sensor. Slug and stratified flow experiment are carried out in this study, and the evaluation of the test results by the classical void fractions model proves that the sensor has high measurement accuracy.

2. Void fraction measurement principle

2.1 Analysis of dielectric polarization effects

The electromagnetic waves with very high frequency (30-300 MHz) belong to invisible light, and their energy propagates in the form of photons. According to the electromagnetic field theory, the dielectric will be polarized under the effect of the alternating electric field generated by electromagnetic field excitation. Non-polar molecules (air, natural gas, etc.) and polar molecules (water) in the electromagnetic field have different polarization effects, accompanied by the attenuation of the dielectric constant. Turning polarization occurs in polar molecules (water) that are subjected to excitation of a high-frequency electromagnetic field, which causes severe loss of dielectric constant. In contrast, non-polar molecules (air and natural gas) undergo only displacement polarization with zero dielectric constant loss [13]. Therefore, the measurement of gas-liquid components can be distinguished by the change of the dielectric constant ε.The dielectric constant ε is also a function of the frequency of the electromagnetic wave, and its complex form is：

$$\varepsilon(\omega) = \varepsilon'(\omega) - j\varepsilon''(\omega) \qquad (1)$$

Where ω denotes the electromagnetic wave propagation frequency. The ε' the real part of the complex permittivity, which corresponds to the capacitance term and represents energy storage. The ε'' is the imaginary part of the complex permittivity, which corresponds to the inductance term and represents the dissipation of energy. The value of the loss angle tangent function is:

$$\tan\theta = \frac{\varepsilon''}{\varepsilon} = \frac{\dfrac{\left(\varepsilon_{(0)} - \varepsilon_\infty\right)\omega\tau}{1+\omega^2\tau^2} + \dfrac{\sigma}{\omega\varepsilon_0}}{\omega\left(\varepsilon_\infty + \dfrac{\left(\varepsilon_{(0)} - \varepsilon_\infty\right)}{1+\omega^2\tau^2}\right)} \qquad (2)$$

where τ is the time constant of turning polarization in dipole, and $\tau = 10^{-9}$s. $\varepsilon_{(0)}$ is the relative permittivity at static, $\varepsilon_{(\infty)}$ is the relative permittivity when $\omega \to \infty$, ε_0 is the permittivity of the vacuum (F/m), and σ is the complex conductivity (m/s).

As can be seen in formula (2), although the energy storage capacity of the dielectric is proportional to the frequency, it is little affected by the frequency. The imaginary part of the dielectric constant tends to rise linearly with frequency, and its change can reflect the change of the dielectric constant.

When the electrostatic field $\omega = 0$, $\tan\theta$ tends to infinity, and the loss formula has no practical meaning. When the high-frequency electromagnetic wave propagates in the coaxial line, the phase difference caused by the loss has a physical meaning, and Eq. (2) is simplified as:

$$\tan\theta \approx \frac{\sigma}{\left(\omega\varepsilon_0\varepsilon_{gw}\right)} \qquad (3)$$

Where ε_{gw} denotes the relative dielectric constant of mixed media.

2.2 Electromagnetic wave propagation characteristics

According to the electromagnetic field theory, the propagation coefficient γ is a parameter that characterizes the variation of electromagnetic waves in a gas-liquid two-phase flow，which be expressed as：

$$r = j\omega\sqrt{\mu_0\varepsilon_0\left(\varepsilon' - j\varepsilon''\right)} = \alpha + j\beta \qquad (4)$$

Where μ_0 is the permeability of vacuum (H/m), then attenuation constant α and phase constant β of coaxial line can be derived from Eq. (3) and Eq. (4)

$$\alpha = \sqrt{\frac{\omega^2\mu_0\varepsilon_0\varepsilon_{gw}}{2}\left[\sqrt{1+\tan^2\theta} - 1\right]^{\frac{1}{2}}} \qquad (5)$$

$$\beta = \sqrt{\frac{\omega^2\mu_0\varepsilon_0\varepsilon_{gw}}{2}\left[\sqrt{1+\tan^2\theta} + 1\right]^{\frac{1}{2}}} \qquad (6)$$

2.3 Principle of phase difference measurement

When the electromagnetic wave propagation in the coaxial line, it is clear that the value of the propagation coefficient γ mainly depends on the relative permittivity and conductivity of the gas-liquid two-phase mixed media as shown in Eq. (4).

The attenuation coefficient α is used to measure the effect of mineralization on the media, and the phase constant β is used to characterize the void fraction. when ω is large enough, then

$$\tan\theta = \frac{\sigma}{\omega\varepsilon_0\varepsilon_{gw}} \ll 1 \qquad (7)$$

The equation (6) is simplified as:

$$\beta = \omega\sqrt{\mu_0\varepsilon_0\varepsilon_{gw}} \qquad (8)$$

Then the phase shift produced by the electromagnetic wave is

$$\Delta\varphi = L\beta \qquad (9)$$

where L and $\Delta\varphi$ denote the coaxial line length and phase shift. When the electromagnetic wave frequency is certain the phase is only determined by the dielectric coefficient of the mixed medium.

$$\Delta\varphi = \omega L\sqrt{\mu_0\varepsilon_0\varepsilon_{gw}} \qquad (10)$$

The dielectric constant is chosen in series because of the vertical electric field direction at the gas-liquid interface in the stratified and slug flow conditions. In dynamic measurement, the mixed dielectric constant of the gas-liquid mixture is:

$$\varepsilon_{gw} = \frac{\varepsilon_w\varepsilon_g}{\varepsilon_w\alpha_g + \varepsilon_g\alpha_w} \qquad (11)$$

Water is a strongly polar liquid medium, in the electric alternating electric field under the action of dipole turning polarization plays a major role. Its dielectric constant varies as a function of temperature as:

$$\varepsilon_w = -0.37T + 87.80 \qquad (12)$$

3. Sensor and Experiment

3.1 Structure design of sensor

The coaxial line phase measurement sensor based on electromagnetic wave measurement principle is shown in Fig.1. The inner electrode is made of copper conductor, which passes through a U-shaped tube with the length of 180mm in the bottom. The U-shaped tube is welded with

test pipe to prevent fluid leakage, and the coaxial line is located on the central axis of the pipe. The exterior electrode is fixed on the test pipe with the ID is 50mm.
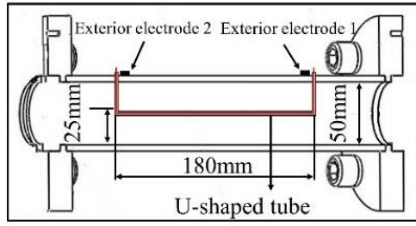

Figure.1 The coaxial line phase sensor

When the electromagnetic wave propagates in the coaxial line, an electromagnetic field is formed between the U-tube and the test pipe section as shown in Figure 2. Electromagnetic waves are transmitted in (Transverse Electric and Magnetic Field TEM) mode, where the electric and magnetic fields are radiated in the coaxial line cross-section. The TEM mode has the advantage of structural stability and the shielding effect of the outer conductor that prevents the electromagnetic field from being disturbed by the external environment. The electromagnetic wave is transmitted to the phase discriminator through internal and external electrodes, and the intensity of the electromagnetic wave signal is attenuated when passing through the mixing medium. The mixed dielectric constant changes with two-phase component and medium physical parameters.
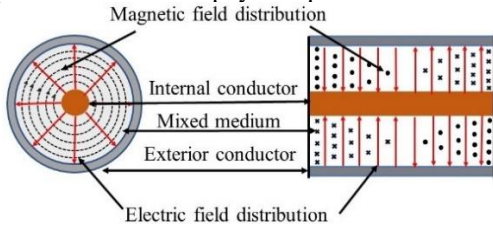

Fig.2 Electromagnetic field distribution in sensor

3.2 Phase difference measurement system
The void fraction measurement system based on coaxial line phase sensor is shown in Fig.3. The micro-controller STM32F103 sends instructions to signal generator AD9959 through the SPI bus, and AD9959 generates a 115MHz electromagnetic wave. The electromagnetic wave is divided into two equal and independent signals by the power divider. One of them is sent to the interior and exterior electrode of the coaxial line phase sensor simultaneously, while the other electromagnetic wave signal is transmitted directly to the phase discriminator AD8302 as a reference. The exterior and interior electrode 1 is connected to the power divider, while the exterior and interior electrode 2 are connected with the phase discriminator. The output phase difference signal is measured by amplitude discriminator AD8302 and converted to a voltage signal, which is acquired by a 12bit AD converter integrated into STM32F103 and transmitted to the master computer.
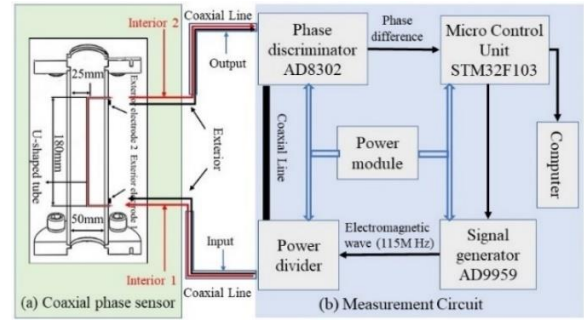

Figure.3. Coaxial line measurement system

The phase discriminator AD8302 receives two input signals from the power divider and electrode of the coaxial line respectively. Two broadband logarithmic detectors integrated into AD8302 realize the precision matching of two input channel signals, which are converted to voltage signal. the expression is

$$V_{OUT} = V_{SLP} Log(V_{INA} / V_Z) \quad (13)$$

Where, V_{IN} and V_Z are the input signal and intercept respectively, and the output value is zero when their values are equal. The slope V_{SLP} represents the parameter of a logarithmic amplifier. The output signal is processed by a multiplicative phase detector together the output result becomes

$$V_{MAG} = V_{SLP} Log(V_{INA} / V_{INB}) \quad (14)$$

By the using of logarithmic amplifier and multiplicative phase detector in AD8302, the phase output form is obtained as follows

$$V_p = V_\phi \left[\phi(V_{INA}) - \phi(V_{INB}) \right] \quad (15)$$

V_ϕ is the slope and is the parameter of the logarithmic amplifier, and V_{INA} and V_{INB} come from reference phase and electrode of coaxial respectively. The signal is processed by output amplifier, feedback circuit and so on, the signal amplitude and phase are measure as follows

$$V_{MAG} = R_F I_{SLP} Log(V_{INA} / V_{INB}) + V_{CP} \quad (16)$$

$$V_{PHS} = -R_F I_\varphi \left[\left| \phi(V_{INA}) - \phi(V_{INB}) - \frac{\pi}{2} \right| \right] + V_{CP} \quad (17)$$

Where, the slope of phase measurement represented by $R_F I_\varphi$ is 10mV/°, V_{CP} stands for the center point, the phase corresponding to the center point 900mV is 90°, and the phase difference range from 0° to 180° degrees correspond to the output voltage range from 0 to 1.8 V.

3.3 Experimental design of two-phase flow
The laboratory test was conducted on a double closed-loop gas-liquid two-phase flow experimental device (with the ID 50mm in test pipe) at the National and Local Joint Engineering Research Centers of Metrology Instruments and Systems of Hebei University. The coaxial line phase sensor Fig. 4 (a) connected to the experimental devices Fig. 4 (b) main via a flange. The experimental fluid was water and compressed air. The device adopts a double-loop circuit design, and gas-liquid can be opened and flow regulated independently by their respective electric switching valves and regulating valves.

The gas circuit consists of two branches, and the liquid circuit consists of two branches that can be opened independently or used in combination according to the condition of liquid flow rate. The water enters the front of the experimental tube section mix with the water. The gas-liquid two-phase flow is fully developed by 260D and then passed through the horizontal test pipe section. The temperature and pressure of each phase at each observing point were recorded together with two-phase flow parameters by the data acquisition system in the further data processing.

(a) Coaxial phase sensor

(b) Schematic of two-phase flow circulation system
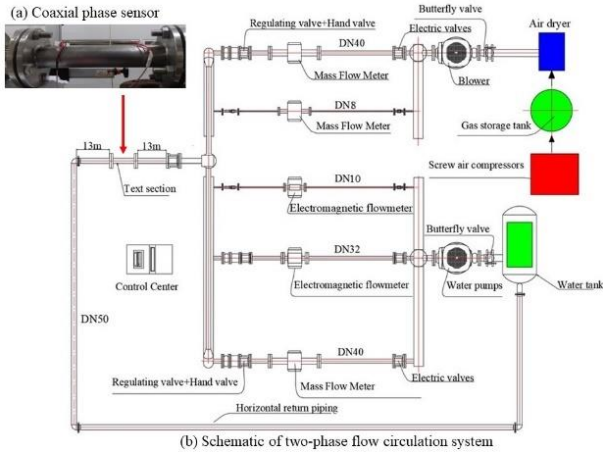
Figure. 4. Experimental setup of two-phase flow

The desired flow rates of both water and air were then circulated in the system via the corresponding control valves until a steady-state condition was reached. The data collection with a sampling frequency of 20 Hz after the flow stabilizes for 2 minutes. All the experiment are conducted at room temperature and pressure, and the range of experimental parameters is shown in Table 1.

Table 1 Range of experimental parameters

Flow pattern	u_{sg} (m/s)	u_{sl} (m/s)	Points
Slug	0.071-1.132	0.057~1.415	63
Stratified	0.085-0.566	0.111~0.198	60

4. Experiment results and analysis

4.1 Void fraction measurement result

Randomly intercepted 4s data of void fraction are plotted against time are shown in Fig 5. Under the condition of u_{sl}=0.707m/s, the variation curves of the void fraction are shown in Figure. 5, the void fraction of the slug flow varies periodically with time, which consistent with the intermittently characteristics of slug flow. It can be seen that when the liquid plug appears, the void fraction is maintained at a low value. Nevertheless, the void fraction is not equal to zero for the reason that numbers of bubbles be entrained in the liquid plug. The void fraction is maintained at a high value when a large gas bullet is present. It can also be seen from the figure that as the gas

superficial velocity increases, the frequency of gas slug increases, and the void fraction increase as well.
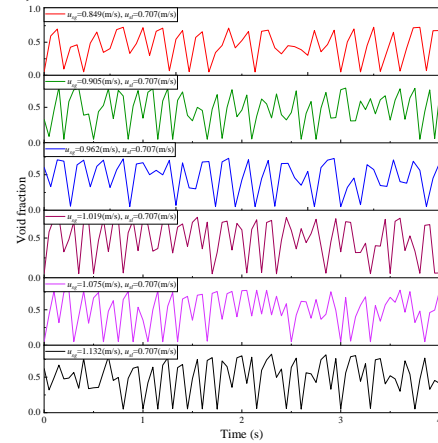

Figure 5: Void fraction time series of slug flow (u_{sl}= 0.707 m /s)
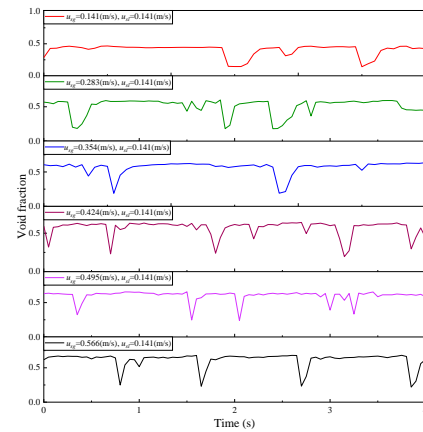

Figure 6: Void fraction time series of stratified flow (u_{sl}= 0.141 m /s)

The void fraction of stratified flow with time is shown in Fig. 5 (b) when the u_{sl}=0.707m/s. Since the velocity of the gas phase is much higher than that of the liquid phase, the gas shearing interaction causes interfacial fluctuations and wave stratified flow occurs. Under the condition of liquid superficial velocity is fixed, the void fraction increases with the increase of superficial velocity u_{sg}, and the frequency of interfacial fluctuation also shows an increasing trend.

Calculate the Probability Density Functions (PDF) of void fraction at the same condition of Fig.5. Shapes of PDF profiles changes for different flow patterns. Two peaks are observed in the PDF profiles for slug flows in Fig.7, while only one peak exists for the stratified flow in Fig.8. For the slug flow, the highest PDF is obtained when α is around zero, this means that the cross section is occupied by the liquid phase for most time. Another crest is are relatively smaller compared with the first one, which corresponds to cases when middle part of the gas slug pass through the cross section with a constant liquid film. For the stratified flow, the gas phase exists along the flow domain, resulting in the disappearance of the first peak of PDF profiles. The shape of PDF is an efficient

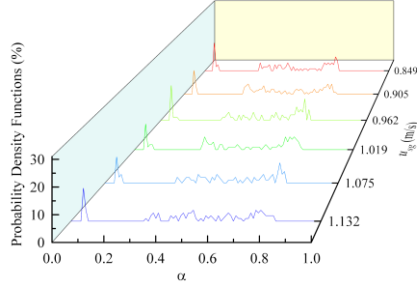way to distinguish intermittent flows from separated flows.

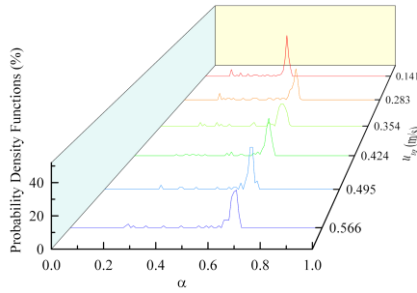Figure 7: PDF distributions for slug flow (u_{sl}= 0.707 m /s)

Figure 8: PDF distributions for stratified flow (u_{sl}= 0.141 m /s)

4.2 Measurement accuracy evaluation

In order to evaluate the measurement accuracy of coaxial line phase sensor, the classical void fraction predicted correlation were selected to compare with the experiment data.

Woldesemayata and Ghajar [14] had compared the 68 representative void fraction models in resent research of two-phase flow, which are classified into homogeneous flow slip ratio, drift flux, and General correlations employed the available experimental data to validate and evaluate these models. Armand–Massina [14] based on homogeneous flow correlation is obtained by improving on Armand correlation, which is:

$$\alpha_g = (a+bx)k_\varepsilon \qquad (18)$$

$$k_\varepsilon = \frac{1}{1+\frac{1-x}{x}\times\frac{\rho_g}{\rho_l}} \qquad (19)$$

Where，α_g is void fraction，x is gas quality factor, ρ_g and ρ_l are the density of gas and liquid, respectively.

Kanizawa and Ribatski (2016)[15] developed the slip ratio correlation as a function of the dryness fraction x, Froude number of the mixture F_{rm}, and the density ratio of gas and liquid (ρ_g/ρ_l) based on minimum kinetic energy, which is described as:

$$\varepsilon = \left(1+1.021 F_{rm}^{-0.092}\left(\frac{\mu_l}{\mu_g}\right)^{-0.368}\left(\frac{\rho_g}{\rho_l}\right)^{1/3}\left(\frac{1-x}{x}\right)^{2/3}\right)^{-1} \qquad (20)$$

$$F_{rm} = \frac{G^2}{(\rho_l-\rho_g)^2 gD} \qquad (21)$$

$$G = u_{sg}+u_{sl} \qquad (22)$$

Where G is Mass velocity, μ_g and μ_l are dynamic viscosity of gas and liquid, respectively. Rassame and Hibiki (2018)[16] proposed a drift-flow correlation method that was used to predict the void fraction of gas-liquid two-phase flow in horizontal pipe due to its simplicity and practicality.

$$a = \frac{u_{sg}}{C_0 G+u_{gi}} \qquad (23)$$

$$C_0 = \begin{cases} 0.8\exp\left(0.815\left(\frac{\langle j_g^+\rangle/\langle j^+\rangle}{0.9}\right)^{1.5}\right) - \left[0.8\exp\left(0.815\left(\frac{\langle j_g^+\rangle/\langle j^+\rangle}{0.9}\right)^{1.5}\right)-1\right]\sqrt{\frac{\rho_g}{\rho_l}}, & 0<\left(\langle j_g^+\rangle/\langle j^+\rangle\right)\le 0.9 \\ \left(-8.08\langle j_g^+\rangle/\langle j^+\rangle+9.08\right)-8.08\left(\langle j_g^+\rangle/\langle j^+\rangle+1\right)\sqrt{\frac{\rho_g}{\rho_l}}, & 0.9\le\left(\langle j_g^+\rangle/\langle j^+\rangle\right)\le 1 \end{cases} \qquad (24)$$

$$\langle j_g^+\rangle = \frac{\langle j_g\rangle}{\left(\frac{\Delta\rho g\sigma}{\rho_l^2}\right)^{\frac{1}{4}}} \qquad (25)$$

$$\langle j^+\rangle = \frac{\langle j\rangle}{\left(\frac{\Delta\rho g\sigma}{\rho_l^2}\right)^{\frac{1}{4}}} \qquad (26)$$

Huq and Loth (1992)[17] derived an analytical formula without empirical constants utilizing the methodology of data fitting, which is defined as:

$$a = 1-\frac{2(1-x)^2}{1-2x+\left[1+4x(1-x)\left(\frac{\rho_g}{\rho_l}-1\right)\right]^{0.5}} \qquad (27)$$

The agreement between measurement accuracy of coaxial line phase sensor and the empirical model available in above literatures compared by mean absolute percentage error (MAPE), defined as,

$$\text{MAPE} = \frac{1}{N}\sum_{i=1}^{N}\frac{\left|\langle y_{cor,i}\rangle-\langle y_{exp,i}\rangle\right|}{\langle y_{exp,i}\rangle}\times 100\% \qquad (28)$$

Where N, $y_{cor,i}$ and $y_{exp,i}$ are the points of data, correlate value, and measured value, respectively.
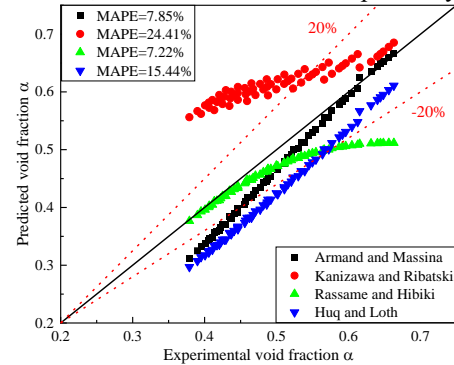

Figure 9: Measurement accuracy of slug flow

The comparison between the experimental data measured by coaxial line phase sensor and the void fraction drived by literature correlations as shown in Fig. 9 and 10. The MAPE of the selected correlations are 7.85%, 24.41%, 7.22%, and 15.44%, respectively. The results in Fig.9 indicated that the models with different theoretical backgrounds have different prediction results for the void fraction, and the drift flux model has the highest prediction accuracy in slug regime. The MAPE of these

correlations that predicted in stratified regime are 12.31%, 6.46%, 12.68%, and 2.95%, respectively, as shown in Fig.10. The results show that the measured values of void fraction under stratified flow conditions are in good agreement for all selected models.
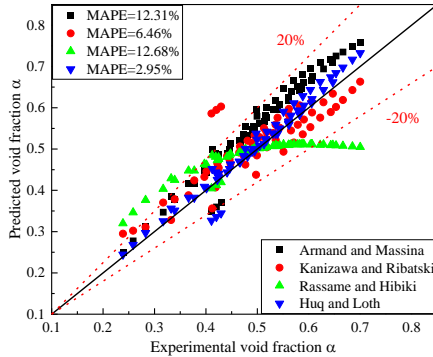

Figure 10: Measurement accuracy of stratified flow

5. Conclusion

(1) A coaxial line phase sensor is designed based on the electromagnetic wave propagation principle in this paper, which has the advantages of wide range of application, real-time, and simple structure.

(2) The time-domain and Probability Density Functions (PDF) distribution show that the sensor can reflects dynamic characteristics of void fraction effectively.

(3) The measurement accuracy evaluated by four empirical correlations with different physical backgrounds indicated that the sensor has well measurement accuracy and not limited by the flow regime.

References

[1] R. Kong, Q. Zhu, S. Kim, M. Ishii, S. Bajorek, K. Tien, C. Hoxie, Void fraction prediction and one-dimensional drift-flux analysis for horizontal two-phase flow in different pipe sizes, Experimental Thermal and Fluid Science 99 (2018) 433-445.

[2] N. Mithran, M. Venkatesan, Volumetric Reconstruction of Taylor Slug Gas Flow Using IR Transceiver in Minichannels, IEEE Transactions on Instrumentation and Measurement 69(6) (2020) 3818-3825.

[3] L. Wangxu, L. Zhenggui, D. Wanquan, J. Lei, Q. Yilong, C. Huiyu, Particle image velocimetry flowmeter for natural gas applications, Flow Measurement and Instrumentation 82 (2021).

[4] C. Corazza, K. Rosseel, W. Leysen, K. Gladinez, A. Marino, J. Lim, A. Aerts, Optical fibre void fraction detection for liquid metal fast neutron reactors, Experimental Thermal and Fluid Science 113 (2020).

[5] N. Zhao, C. Li, H. Jia, F. Wang, Z. Zhao, L. Fang, X. Li, Acoustic emission-based flow noise detection and mechanism analysis for gas-liquid two-phase flow, Measurement 179 (2021).

[6] D.S. van Putten, B.T. Dsouza, Wet gas over-reading correction for ultrasonic flow meters, Experiments in Fluids 60(3) (2019).

[7] S.A. Mäkiharju, C. Gabillet, B.-G. Paik, N.A. Chang, M. Perlin, S.L. Ceccio, Time-resolved two-dimensional X-ray densitometry of a two-phase flow downstream of a ventilated cavity, Experiments in Fluids 54(7) (2013).

[8] M. P, V.M. S, Void-fraction reconstruction with stochastic data, Experiments in Fluids 16 (1994) 217-222.

[9] D.J. Euh, B.J. Yun, C.H. Song, Benchmarking of the five-sensor probe method for a measurement of an interfacial area concentration, Experiments in Fluids 41(3) (2006) 463-478.

[10] M. Abdulkadir, B. Ugwoke, L.A. Abdulkareem, D. Zhao, V. Hernandez-Perez, Experimental investigation of the characteristics of the transition from spherical cap bubble to slug flow in a vertical pipe, Experimental Thermal and Fluid Science 124 (2021).

[11] D.V. Blackham, R.D. Pollard, An Improved Technique for Perimittivity Measurements Using a Csaxial Probe, IEEE TRANSACTIONS ON INSTRUMENTATION AND MEASUREMENT (1997) 1093-1099.

[12] C. Zhao, G. Wu, Y. Li, Measurement of water content of oil-water two-phase flows using dual-frequency microwave method in combination with deep neural network, Measurement 131 (2019) 92-99.

[13] X. Chen, Y.F. Han, Y.Y. Ren, H.X. Zhang, H. Zhang, N.D. Jin, Water holdup measurement of oil-water two-phase flow with low velocity using a coaxial capacitance sensor, Experimental Thermal and Fluid Science 81 (2017) 244-255.

[14] M.A. Woldesemayat, A.J. Ghajar, Comparison of void fraction correlations for different flow patterns in horizontal and upward inclined pipes, International Journal of Multiphase Flow 33(4) (2007) 347-370.

[15] F.T. Kanizawa, G. Ribatski, Void fraction predictive method based on the minimum kinetic energy, Journal of the Brazilian Society of Mechanical Sciences and Engineering 38(1) (2015) 209-225.

[16] S. Rassame, T. Hibiki, Drift-flux correlation for gas-liquid two-phase flow in a horizontal pipe, International Journal of Heat and Fluid Flow 69 (2018) 33-42.

[17] R. Huq, J.L. Loth, Analytical two-phase flow void prediction method, Journal of Thermophysics and Heat Transfer 6(1) (1992) 139-144.